Universiteit Antwerpen

This item is the archived peer-reviewed author-version of:

The C_{32} alkane-1,15-diol as a tracer for riverine input in coastal seas

Reference:

Lattaud Julie, Kim Jung-Hyun, De Jonge Cindy, Zell Claudia, Damste Jaap S. Sinninghe, Schouten Stefan.- The C_{32} alkane-1,15-diol as a tracer for riverine input in coastal seas

Geochimica et cosmochimica acta - ISSN 0016-7037 - 202(2017), p. 146-158

Full text (Publisher's DOI): https://doi.org/10.1016/J.GCA.2016.12.030

To cite this reference: https://hdl.handle.net/10067/1424090151162165141

uantwerpen.be

Institutional repository IRUA

Accepted Manuscript

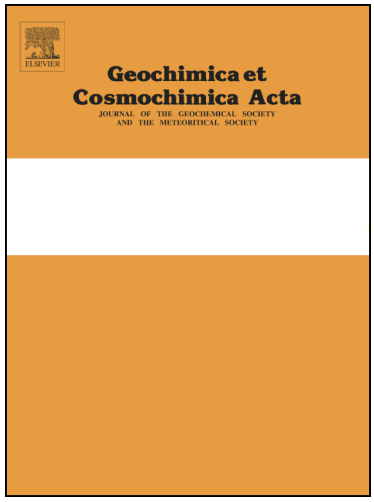

The C_{32} alkane-1,15-diol as a tracer for riverine input in coastal seas

Julie Lattaud, Jung-Hyun Kim, Cindy De Jonge, Claudia Zell, Jaap S. Sinninghe Damsté, Stefan Schouten

PII: S0016-7037(16)30739-6
DOI: http://dx.doi.org/10.1016/j.gca.2016.12.030
Reference: GCA 10082

To appear in: *Geochimica et Cosmochimica Acta*

Received Date: 14 September 2016
Revised Date: 29 November 2016
Accepted Date: 18 December 2016

Please cite this article as: Lattaud, J., Kim, J-H., De Jonge, C., Zell, C., Sinninghe Damsté, J.S., Schouten, S., The C_{32} alkane-1,15-diol as a tracer for riverine input in coastal seas, *Geochimica et Cosmochimica Acta* (2016), doi: http://dx.doi.org/10.1016/j.gca.2016.12.030

This is a PDF file of an unedited manuscript that has been accepted for publication. As a service to our customers we are providing this early version of the manuscript. The manuscript will undergo copyediting, typesetting, and review of the resulting proof before it is published in its final form. Please note that during the production process errors may be discovered which could affect the content, and all legal disclaimers that apply to the journal pertain.

ACCEPTED MANUSCRIPT

The C_{32} alkane-1,15-diol as a tracer for riverine input in coastal seas

Julie Lattaud[1*], Jung-Hyun Kim[1†], Cindy De Jonge[1#], Claudia Zell [1 +], Jaap S. Sinninghe Damsté[1,2], Stefan Schouten[1,2]

[1]*NIOZ, Royal Netherlands Institute for Sea Research, Department of Marine Microbiology and Biogeochemistry (MMB), and Utrecht University, Po Box 59, 1790 AB Den Burg, The Netherlands.*

[2]*Utrecht University, Faculty of Geosciences, Department of Earth Sciences, Budapestlaan 4, 3584 CD Utrecht, The Netherlands.*

†Current address: Korea Polar Research Institute, 26 Songdomirae-ro, Yeonsu-gu, Incheon 21990, South Korea

#Current address: Department of Biology, Antwerpen University, Campus Drie Eiken, Universiteitsplein 1-610 Wilrijk, Belgium.

+ Current address: Département Biogéochimie, Pierre and Marie Curie University, UMR 7619 METIS, 4 place Jussieu, 75252 Paris, France.

**Corresponding author: Julie.lattaud@nioz.nl*

Resubmitted to *Geochimica et Cosmochimica Acta*

ACCEPTED MANUSCRIPT

ABSTRACT

Long chain alkyl diols are lipids that occur ubiquitously in marine sediments and are used as a proxy for sea surface temperature (SST), using the Long chain Diol Index (LDI), and for upwelling intensity/high nutrient conditions. The distribution of 1,13- and 1,15-diols has been documented in open marine and lacustrine sediments and suspended particulate matter, but rarely in coastal seas receiving a significant riverine, and thus continental organic matter, input. Here we studied the distribution of diols in four shelf seas with major river outflows: the Gulf of Lion, the Kara Sea, the Amazon shelf and the Berau delta, covering a wide range of climate conditions. The relative abundance of the C_{32} 1,15-diol is consistently higher close to the river mouth and particularly in the suspended particulate matter of the rivers suggesting a terrigenous source. This is supported by statistical analysis which points out a significant positive correlation between the C_{32} 1,15-diol and the Branched and Isoprenoid Tetraether index, a proxy reflecting soil and riverine input in marine environments. However, the C_{32} 1,15-diol was not detected in soils and is unlikely to be derived from vegetation, suggesting that the C_{32} 1,15-diol is mainly produced in rivers. This agrees with the observation that it is a dominant diol in most cultivated freshwater eustigmatophyte algae. We, therefore, suggest that the relative abundance of the C_{32} 1,15-diol can potentially be used as a proxy for riverine organic matter input in shelf seas. Our results also show that long chain alkyl diols delivered by rivers can substantially affect LDI-reconstructed SSTs in coastal regions close to river mouths.

ACCEPTED MANUSCRIPT

ACCEPTED MANUSCRIPT

1.Introduction

Long chain alkyl diols (LCD) are molecules composed of a long alkyl chain (number of C atoms ≥28) containing alcohol groups at C_1 and at a mid-chain position (e.g. carbon number 12, 13, 14, 15), which have been reported in a wide range of environments (de Leeuw et al.,1979; Versteegh et al., 1997, 2000; Gogou and Stephanou 2004; Schmidt et al. 2010; Rampen et al., 2012, 2014b; Romero-Viana et al., 2012; Plancq et al., 2015; Zhang et al., 2011 and references therein). In marine environments, the major LCDs are typically C_{28} and C_{30} 1,13-diols, C_{28} and C_{30} 1,14-diols, and C_{30} and C_{32} 1,15-diols (Rampen et al., 2014a). C_{28} and C_{30} 1,14-diols are biosynthesized by the diatom genus *Proboscia* (Sinninghe Damsté et al., 2003, Rampen et al., 2007) and the marine algae *Apedinella radians* (Rampen et al., 2011), while C_{28} and C_{30} 1,13-diols and C_{30} and C_{32} 1,15-diols have been reported in eustigmatophyte algae (Volkman et al., 1992, 1999; Gelin et al., 1997; Méjanelle et al., 2003). However, eustigmatophyte algae are rarely reported in the marine environment and the distribution of diols present in marine eustigmatophyte algae (genus *Nannochloropsis*) does not match with the diol distribution in marine environments (Volkman et al., 1992; Versteegh et al., 1997; Rampen et al., 2014a).

Multiples indices using LCDs have been developed that reflect different environmental parameters in the marine environment. One such index is the LDI (Long chain Diol Index, equation 1, [C_{30} 1,15] stands for fractional abundance of the diol), which is used as a proxy for Sea Surface Temperature (SST; Rampen et al., 2012):

$$LDI = \frac{[C_{30}1,15]}{[C_{30}1,15]+[C_{30}1,13]+[C_{28}1,13]} \quad (1)$$

The LDI of marine surface sediments shows a strong correlation (r^2=0.97) with SST (between -3°C and 27°C). Another index is diol index 1 (equation 2) which has been developed by Rampen et al. (2008) to trace upwelling conditions.

ACCEPTED MANUSCRIPT

$$diol\ index\ 1 = \frac{[C_{30}1,14]+[C_{28}1,14]}{[C_{30}1,14]+[C_{28}1,14]+[C_{30}1,15]} \quad (2)$$

This index is based on the fractional abundance of C_{30} 1,14- and C_{28} 1,14- diols, produced primarily by *Proboscia* diatoms. As *Proboscia* diatoms thrive in upwelled, nutrient-rich water they are a good indicator of upwelling conditions. This upwelling index has been applied for the upwelling region of the Arabian Sea (Somalian upwelling; Rampen et al., 2008). Willmott et al. (2010) constructed another diol index (diol index 2, equation 3) as a proxy for paleo productivity of *Proboscia* diatoms and upwelling intensity at high latitudes (around the Antarctic peninsula).

$$diol\ index\ 2 = \frac{[C_{30}\ 1,14]+[C_{28}1,14]}{[C_{30}\ 1,14]+[C_{28}\ 1,14]+[C_{30}\ 1,13]+[C_{28}\ 1,13]} \quad (3)$$

Rampen et al. (2014a) studied these two indices in globaly distributed marine sediments and showed that the diol index 1 is likely impacted, besides by upwelling and high nutrients, by SST, while the diol index 2 is more widely applicable as an indicator of upwelling conditions. Another diol index (diol index 3, equation 4) has been created for the Congo River fan by Versteegh et al. (1997, 2000) to assess relative changes in salinity.

$$diol\ index\ 3 = \frac{[C_{30}1,15]}{[C_{30}1,15]+[C_{32}1,15]} \quad (4)$$

However, Rampen et al. (2012) showed that, on a global scale, this diol index only had a weak correlation with salinity (Pearson correlation $r<0.3$).

With respect to freshwater environments, Rampen et al. (2014b) showed that the LDI in surface sediments of lakes only correlated weakly with mean annual air temperature (a proxy for lake surface temperature) and that the distributions of LCDs differ from those in marine sediments. This indicates that the producers and environmental controls on diols in lakes are different compared to those in marine environments. Interestingly, only a few studies have investigated the diol distributions in marine

ACCEPTED MANUSCRIPT

environments affected by continental input, i.e near large river outflows. A recent study by De Bar et al. (2016) on long chain diol distributions of the Portugese margin suggested that some diols, in particular the C_{32} 1,15-diol, may be partially derived from a continental source. Indeed, Rampen et al. (2014a) also reported relatively high amounts of the C_{32} 1,15-diol in several estuarine sediments and Versteegh et al. (1997) showed that this diol was relatively more abundant close to the river mouth of the Congo River, suggesting also a partial source from the continent. However, it is unclear if the C_{32} 1,15-diol is consistently derived from continental sources in coastal seas and from which sources on the continent the C_{32} 1,15-diol is derived.

To constrain the distribution and origin of the C_{32} 1,15-diol in coastal marine environments, we studied four coastal seas with a substantial river input and from different climate zones: The Gulf of Lion and the Rhône River (Mediterrannean Sea) with a temperate climate, the Amazon shelf and the Amazon River (Atlantic Ocean) and Berau delta region (Pacific Ocean) with a tropical climate, and the Yenisei River and Kara Sea (Arctic Ocean) with a (sub)polar climate (Fig. 1). Our results shed light on the origin of the C_{32} 1,15-diol in coastal seas and suggest its potential as a proxy for the input of riverine organic matter (OM).

2. Material and Methods

2.1 Study sites and sampling

2.1.1 Gulf of Lion

The Gulf of Lion is located in the northwestern part of the Mediterranean Sea (42°N 3°E and 44°N 6°E; Fig. 1) with a fairly broad and crescent shaped continental shelf and is under the strong influence of rivers. The major river discharging into the Gulf of Lion is the Rhône River, with a catchment area of 98 000 km^2 and a length of 813 km. Its source is the Rhône glacier in the Swiss Alps. The river is

ACCEPTED MANUSCRIPT

subsequently discharged through the Lake Geneva and southern France into the Gulf of Lion (Mediterranean Sea). The average water discharge is ca. 1.7 x 10^3 m^3/s (Thill et al., 2001), and a mean sediment discharge of 7-10 x 10^6 tons/yr represents 80 % of the inflow into the Gulf of Lion (Durrieu de Madron et al., 2000, Sabatier et al., 2006). Other rivers besides the Rhône River which discharge into the Gulf of Lion are the Vidourle, Herault, Orb, Aude, Agly, Têt and Tech rivers in France and the Riu Ter, Fluvia and Tordera rivers in Spain. These rivers have more episodic discharges corresponding with major rainfalls associated with storms. The major current in the Gulf of Lion is the Liguro-Provencal going from East to West. The Mediterranean climate is characterized by warm, dry summers and mild to cool, wet winters. The mean annual sea surface temperature (SST) is ranging from 16°C to 19°C (Kim et al., 2015). The mean annual air temperature (MAAT) in the Rhone catchment is 9°C (Olivier et al., 2009).

The Gulf of Lion sample set consisted of 50 surface (0-0.5 or 0-1 cm) sediments and one sample of suspended particulate matter (SPM) of the Rhône river. The samples were previously studied for Glycerol Dialkyl Glycerol Tetraether (GDGT) lipids and bulk parameters by Kim et al. (2006, 2007, 2010, 2014, 2015). The surface samples have been collected during several French research programs (River-Dominated Ocean Margins, Climate and Human-Induced Alterations in Carbon Cycling at the River–Sea Connection) and research programs funded by the European Union (Hotspot Ecosystem Research on the Margins of European Seas, European Margin Strata Formation). The SPM was collected close to the water surface in the Rhône River: 5 l of water were filtered through pre-ashed glass fiber filters (Whatman GF-F, 0.7 µm, 142 mm diameter) with an in-situ pump system (WTS, McLane Labs, Falmouth, MA). All samples were kept frozen at -20°C and freeze dried before analysis.

2.1.2 Amazon shelf

The Amazon River is the largest drainage system in the world (6.1 × 10^6 km^2) in term of fresh-water discharge (Milliman and Meade 1983) and catchment area (Goulding et al., 2003). Both its main (the

ACCEPTED MANUSCRIPT

Madeira River) and secondary (the Solimoes River) tributaries originate in the Bolivian Andes. Due to the equatorial position, the temperature in the drainage basin is relatively constant year-round with a MAAT of 26°C (New et al., 2002). The coldest temperature is in the Andes Mountains due to the high elevation. The mean annual water discharge is 2 x 10^5 m^3/s at Óbidos (Callede et al., 2000) and the mean annual sediment discharge is 8-12 x 10^{11} kg/yr (Dunne et al., 1998). The mean annual SST for the Atlantic Ocean offshore the Amazon River mouth is 28°C (Zell et al., 2014).The major current on the Amazon shelf is the North Brazilian Current, transporting riverine suspended matter to the northwest, along the North Brazilian coast.

From the Amazon region, 14 marine surface sediments and 36 samples of riverine SPM (Fig. 1) were collected as described by Zell et al. (2014). These samples have been previously studied for GDGTs by Kim et al. (2012), Zell et al. (2013a, 2013b, 2014) and for long chain glycolipids by Bale et al. (2015). Surface sediments of the Amazon shelf and slope were collected on board of the R/V Knorr, cruise 197-4 between February and March 2010. All sediment samples were freeze dried prior to analyses. SPM was collected along the Amazon River main stem, in four tributaries (Solimones, Negro, Madeira, and Tapajos), and in five varzeas (Cabaliana, Janauaca, Marituba, Canacari, and Curuai). All SPM samples were kept frozen at -20°C and freeze dried before analysis.

2.1.3 Yenisei River and Kara Sea

The Yenisei River is the ninth largest river in the world in terms of discharge (Telang et al., 1991), and it crosses Mongolia and Siberian Russia in a south to north direction covering different climate zones. Thus, the Yenisei river watershed is characterized by large differences in MAAT, i.e. -6°C in the southern part of the catchment dropping to -11.4°C in the most northern parts (De Jonge et al., 2014). The mean annual discharge is estimated at 2 x 10^4 m^3/s. The Yenisei River catchment area is approximately 2.6 x 10^6 km^2. It

ACCEPTED MANUSCRIPT

discharges into the Kara Sea, which is the second largest shelf area of the Arctic Ocean. A fifth of the continental run-off of the Eurasian continent drains into the Kara Sea (Lammers et al., 2000), where the Ob and Yenisei rivers provide the largest part of the water discharge. The two rivers are separated by the Gydan peninsula. The Yenisei discharge and Kara Sea circulation are characterized by a strong seasonality. During the summer months, the surface currents in the Kara Sea follow a cyclonic circulation. From mid-October to mid-May the Kara Sea and Yenisei River estuary are almost entirely ice-covered. The mean annual SST for the Kara Sea is -1°C (Boyer et al., 2013).

SPM from the Yenisei river water (16 river SPM) and the Kara Sea (21 surface sediments, Fig. 1) were obtained as described by De Jonge et al. (2014) by filtrating water through a GF/F glass fiber filter (0.7 µm pore size) using a McLane in-situ pump. For some sites in the Kara Sea, surface sediments were obtained via box coring on the R/V Akademik Mstislav Keldysh. These samples have been previously studied for GDGTs and bulk parameters by De Jonge et al. (2014, 2015a, 2015b).

2.1.4 Berau delta

The Berau delta is situated along the east coast of Kalimantan (Indonesia) and is a coastal and shallow embayment. It is situated north of the Makassar Trait, which is one of the main passages between the Indian Ocean and Pacific Ocean. The catchment area of the Berau River, which accounts for most of the freshwater input, is estimated at $1x10^4$ km^2 (Booij et al., 2012) and the area of the delta is about 800 km^2 (Sinninghe Damsté, 2016). Kalimantan has a tropical climate with a dry season from May to October and two rainfall seasons: December to January and April to May. The surface water temperature in the Berau delta is relatively constant around 30°C (Arifin and Koesmawati, 2007) and the MAAT in the catchment is around 28°C (Harger, 1995).

A total of 37 surface sediments of the Berau delta were obtained. Samples from transects in the delta were retrieved during a cruise of the R/V Geomarin I in July 2003 and surface sediments (0-5 cm) from

ACCEPTED MANUSCRIPT

stations closer to the river mouth were collected in April 2007 using a Smith-McIntyre grab sampler as described by Booij et al. (2012) and were frozen at -20°C on board (Fig. 1). These samples have been studied previously for polycyclic aromatic hydrocarbons (Booij et al., 2012) and for GDGTs and bulk isotopes (Sinninghe Damsté, 2016).

2.1.5 Soils

Ten soil samples from ten different countries (South Africa, Uruguay, Hawaii, Norway, Honduras, Gabon, France, China, Brazil and Australia) covering a large range of climate zones, were analyzed for long chain diols. These samples are part of the original set of soils used for branched GDGT analysis reported in Weijers et al. (2007), Peterse et al. (2009, 2011) and De Jonge et al. (2014).

2.2 Diol analysis

The surface sediments of the Gulf of Lion have been previously extracted as described in Kim et al. (2006). Briefly, the samples were extracted with an Accelerated Solvent Extractor (DIONEX ASE 200) using a mixture of DCM : MeOH (9 : 1 v/v), and the extracts were separated over an activated aluminium oxide column into three fractions (apolar, ketone and polar). The sediments from the Berau delta were extracted and fractionated in a similar way (see Sinninghe Damsté, 2016). The surface sediments and SPM of the Yenisei basin and Amazon basin have been extracted previously as described in De Jonge et al. (2014) and Zell et al. (2014), respectively. Briefly, the freeze-dried filters and sediments were extracted using a modified Bligh and Dyer method and separated into core GDGT lipids and intact polar lipids over a silica column.

ACCEPTED MANUSCRIPT

The total lipid extracts of 10 soils were base hydrolyzed in 2 mL of 1 N KOH in 96% methanol and refluxed for 1h. After cooling the mixture was centrifuged, and acidified by adding 1mL of 2 N HCl in a H_2O/MeOH mixture. 2 mL of DCM was added followed by centrifugation, and the organic phase was collected. This procedure was repeated 3 times. This extract was separated on an activated aluminum oxide column into three fractions using the following solvents: Hexane : DCM (9 : 1, v/v), Hexane : DCM (1 : 1, v/v) and DCM : MeOH (1 : 1, v/v). The latter (polar) fraction containing the diols was dried under a gentle nitrogen stream.

Diols were derivatized by silylating an aliquot of the polar fraction with 10µL N,O-Bis(trimethylsilyl)trifluoroacetamide (BSTFA) and 10 µL pyridine, heated for 30 min at 60°C and adding 30µL of ethyl acetate. The analysis of diols was performed by gas chromatography-mass spectrometry (GC-MS) using an Agilent 7990B GC gas chromatograph, equipped with a fused silica capillary column (2 5m x 320 µm) coated with CP Sil-5 (film thickness 0.12 µm), coupled to an Agilent 5977A MSD mass spectrometer. The temperature regime for the oven was as follows : 70 °C for 1 min, increased to 130 °C at 20 °C/min, increased to 320 °C at 4 °C/min, held at 320 °C during 25 min. The gas flow was held constant at 2 mL/min. The MS source temperature was held at 250 °C and the MS quadrupole at 150 °C. The electron impact ionization energy of the source was 70 eV. The diols were quantified using Single Ion Monitoring (SIM) of the m/z 299.3 (C_{28} 1,14), 313.3 (C_{28} 1,13, C_{30} 1,15), 327.3 (C_{30} 1,14) and 341.3 (C_{32} 1,15) ions (Versteegh et al., 1997; Rampen et al., 2012). The fractional abundance of the diols is expressed as a percentage of the five diols quantified:

$$\%Diol\ x = \frac{ADiolx}{AC_{32}1{,}15+AC_{30}1{,}15+AC_{28}1{,}13+AC_{30}1{,}13+AC_{30}1{,}14+AC_{28}1{,}14} \times 100 \quad (5)$$

Where A is the peak area of diol and x the diol quantified

ACCEPTED MANUSCRIPT

We calculated the LDI (equation 1) and used the global calibration to obtain the SST as followed (equation 6, Rampen et al., 2012):

$$SST = \frac{LDI - 0.095}{0.033} \quad (6)$$

2.3 Statistical analyses

The data were processed through statistical analysis with the software XLStat 2016. A Principal Component Analysis (PCA) was performed on the fractional abundances of the diol isomers to provide a general view of the variability within the distribution of the diols. Correlations have been evaluated with Pearson r values and considered significant if p values were smaller than 0.005. The average data are reported with their corresponding standard deviation.

3. Results

Sediments from the Gulf of Lion and river SPM from the Rhône River all contained diols with variable distributions (Fig. 2; see Appendix A for values). The C_{30} 1,15-diol was the major diol with 50 % of total diols in the SPM, with the C_{32} 1,15-diol as second most abundant diol (18 %). For most of the marine surface sediments, the C_{30} 1,15-diol was also the dominant diol (average 55 ± 15 % of all diols) followed by the C_{30} 1,14-, C_{32} 1,15- and C_{30} 1,13-diols. The C_{30} 1,15-diol is more abundant in the open marine sediments compared to coastal sediments, which is also the case for the C_{28} 1,13- and C_{28} 1,14-diols (Fig. 3). The C_{32} 1,15-diol comprises 0 to 45 % of diols with a trend towards a higher fractional abundance closer to the coast.

In the Amazon basin the C_{30} 1,15-diol was the dominant diol in marine surface sediments (55 to 90 %), followed by the C_{30} 1,14 (average of 7 ± 3 %, Fig. 2). In the river SPM the C_{32} 1,15-diol (average of 30 ± 22 % reaching up to 76 %) and C_{30} 1,15-diol (average of 20 ± 7 % and reaching up to 47 %) are relatively

ACCEPTED MANUSCRIPT

dominant, while the fractional abundance of C_{32} 1,15-diol in the marine sediments is relatively low (average of 2±1%, Fig. 4).

The C_{32} 1,15-diol (41 ± 18% with values up to 76 %) and C_{30} 1,15-diol (average of 19 ± 16 % and up to 64 % of total diols) are generally the dominant diols in SPM of the Yenisei River and the marine sediments of the Yenisei estuary and Kara Sea (Figs. 2 and 5). The C_{30} 1,13- and C_{28} 1,13-diols were relatively abundant in these samples with a combined average of 26 ± 20 %.

The surface sediments from the Berau delta all contained diols with the C_{30} 1,15-diol being the dominant diol in the sediments further away from the river mouth (average of 68 ± 20 %), while those close to the mouth of the Berau River contained much lower amounts (average of 27 ± 11 %) and relatively high fractional abundances of the C_{32} 1,15- and C_{30} 1,14-diol (average of 18 ± 4 % and 19 ± 10 %, respectively) (Fig. 2). The sediments further away from the coast also have a lower abundance (average of 10 ± 4 %) of the C_{32} 1,15-diol compared to those close to the river mouth (Fig. 6).

4. Discussion

4.1 Distribution of diols in coastal sediments and river SPM

Our study shows that the diol distribution varies substantially within and between the different regions. The Gulf of Lion, Berau delta and Amazon marine surface sediments contain the C_{30} 1,15-diol as the major diol, whereas for the marine surface sediments of the Kara Sea and the Amazon Shelf the C_{32} 1,15-diol is the major diol (Fig. 2). Another interesting feature concerns a latitudinal trend in the proportion of 1,13-diols in marine surface sediments (Fig. 2). The most abundant 1,13-diols are found in surface sediments of the Kara Sea (>30%), followed by the Gulf of Lion and the Berau delta (between 5-20%) and the Amazon basin (<3%), i.e. the colder the SST of the shelf sea, the higher the fractional abundance of

ACCEPTED MANUSCRIPT

the 1,13-diols is found. This is in good agreement with the observations made by Rampen et al. (2012, 2014a), who reported higher relative abundances of 1,13-diols in marine sediments with decreasing sea surface temperatures. The fractional abundance of the C_{32} 1,15-diol is generally higher close to the mouth of the river in all four areas investigated (Figs. 3- 6) and generally the highest in riverine SPM (Fig. 2). For example, for the Amazon shelf, the surface sediments only have a fractional abundance of 2 ± 1 % for the C_{32} 1,15-diol, while in the SPM of the Amazon it amounts 29 ± 22 %.

To confirm the different behavior of the different diols we performed a Principal Component Analysis (PCA, Fig. 7). The first two principal components combined explain 93 and 76 % of the total variance in the distribution of the LCDs for the surface sediments and SPM, respectively. The PCA for the surface sediments shows that for PC1 the C_{30} 1,15-diol is loaded opposite to the C_{28} and C_{30} 1,13-diols which aggregate closely together. This opposite loading is consistent with the behavior of these diols with respect to variations in temperature (cf. Rampen et al., 2012). PC2 of the PCA of the surface sediments separates the 1,14-diols from the other diols, confirming that they are derived from a different source, i.e. *Proboscia* diatoms (Sinninghe Damsté et al., 2003, Rampen et al., 2007). Interestingly, the C_{32} 1,15 diol scores opposite to the C_{30} 1,15-diol on PC1, suggesting a different behavior compared to the C_{30} 1,15 diol. This is even more evident for the PCA of LCD distribution of the riverine SPM where the C_{32} 1,15-diol loads opposite all other diols on PC1. This suggests that the C_{32} 1,15-diol does not have the same source and/or environmental controls as the other diols.

To further investigate the controls on the fractional abundance of the C_{32} 1,15-diol, we investigated the relationships between the fractional abundance of the C_{32} 1,15-diol, annual mean SST, TOC, $\delta^{13}C$ of bulk OM ($\delta^{13}C_{OM}$), BIT index and distance to the river mouth. The $\delta^{13}C_{OM}$ is a proxy for bulk terrigenous versus marine OM (Meyers, 1994) and the BIT index is a proxy for input from continental (riverine and soil) OM into the marine realm (Hopmans et al., 2004; Walsh et al., 2008; Zell et al., 2014 and De Jonge et al.,

ACCEPTED MANUSCRIPT

2015). For this comparison we excluded the 1,14-diols from the data set as the 1,14 diols are known to be produced by another group of organisms (*Proboscia* diatoms; Sinninghe Damsté et al., 2003; Rampen et al., 2007) than the 1,13 and 1,15 diols. Thus, the abundance of C_{32} 1,15-diol was normalized on the sum of all 1,13 and 1,15-diols (equation 7):

$$\%C_{32}1{,}15 = \frac{AC_{32}1{,}15}{AC_{32}1{,}15+AC_{30}1{,}15+AC_{28}1{,}13+AC_{30}1{,}13} \times 100 \quad (7)$$

The results for the combined dataset show no relationship between the percentage of C_{32} 1,15-diol and SST (r = 0.001, p value=0.99; Table 1) agreeing with the conclusion of Rampen et al. (2012). To the contrary, there is a significant positive correlation between C_{32} 1,15-diol and BIT index (r=0.3, p<0.005, Table 1) and a significant negative correlation with $\delta^{13}C_{OM}$ (r=-0.6, p<0.005, Table 1).

On a regional level, the correlation between C_{32} 1,15-diol and BIT index is also observed in the Gulf of Lion and the Berau delta (r= 0.73, p value < 0.005 and r =0.80 p<0.005, respectively) but not for the Kara Sea and Amazon shelf. In the Kara Sea, the BIT index is high in all surface sediments (>0.4), except for the most northern sediments, indicating long-distance transport of soil- and riverine derived OM (De Jonge et al., 2015a). The $\%C_{32}$ 1,15 is showing the same pattern as the BIT, also indicating long-distance transport of material into the Kara Sea (Fig. 5). However, because of soil input from cliffs in the Kara Sea (De Jonge et al., 2015a), the BIT index is also high close to the coast despite a lack of riverine input, while $\%C_{32}$ 1,15-diol is low. Therefore, no significant correlation between BIT index and $\%C_{32}$ 1,15-diol is observed. For the Amazon shelf, the BIT index is low (mostly <0.1) and $\delta^{13}C_{OM}$ values are relatively positive (between -22 and -19‰), suggesting no substantial continental input in these marine sediments. This coincides with a low percentage of C_{32} 1,15-diol (<6%), i.e. much lower than in the other coastal marine sediments and riverine SPM (Fig. 2) and similar to those of open marine sediments (Rampen et al., 2012).

ACCEPTED MANUSCRIPT

Thus, in general the %C_{32} 1,15 is higher close to river mouths, i.e. in sediments with high BIT indices and low $\delta^{13}C_{OM}$ values and, thus, containing a relatively high contribution of terrigenous OM. In contrast, %C_{32} 1,15 is low (<10%) in open marine sediments not containing a substantial terrigenous contribution as evidenced by low BIT index and high $\delta^{13}C_{OM}$values. Together with the substantially elevated amounts of C_{32} 1,15-diol in riverine SPM versus the low amount in nearby marine sediments (Fig. 2), this collectively suggests that the C_{32} 1,15-diol derives, at least in part, from the continent. These results thus confirm the initial observations of De Bar et al. (2016) for surface sediments of the Portuguese margin that %C_{32} 1,15 is higher close to river mouth due to an input from the continent.

4.2 Riverine production of the C_{32} 1,15-diol

To assess if the C_{32} 1,15-diol is derived from riverine production, or transported by rivers from soil or vegetation, we analyzed ten soils from diverse areas for the presence of diols. No 1,13-, 1,14- or 1,15-diols were detected in the examined soils, which implies that, most likely, the presence of C_{32} 1,15-diol in riverine SPM does not originate from soil erosion transporting material originally produced in soil to the river. This is in agreement with Shimokawara et al. (2010) who reported traces of some LCDs (C_{32} 1,17- and C_{34} 1,15-diols) in the surrounding soils of lake Baikal (slopes of the lake) but not the C_{32} 1,15-diol. Furthermore, De Bar et al. (2016) could not detect the C_{32} 1,15-diol in Portuguese soils. Alternatively, the C_{32} 1,15-diol could come from vegetation, as some mid-chain diols (C_{30} to C_{36} 1,ω20-diols) have been reported in land plants and a freshwater fern (Jetter et al., 1996; Jetter and Riederer, 1999; Jetter, 2000; Speelman et al., 2009). However, to the best of our knowledge the C_{32} 1,15-diol has not been reported in higher plants. Thus, by elimination, it seems likely that the C_{32} 1,15-diol is produced in the rivers themselves and subsequently transported to the marine environment.

ACCEPTED MANUSCRIPT

Freshwater eustigmatophyte algae are known to produce the C_{32} 1,15-diol (Volkman et al., 1992, 1999; Rampen et al., 2014b). Within the order Eustigmatophyteae, species of the families Monodopsidaceae and Goniochloridaceae all produce the C_{32} 1,15-diol as a major diol, i.e. with a fractional abundance of 40 - 60% for the Goniochloridaceae and 40 - 80% for the Monodopsidaceae (Rampen et al., 2014b). Furthermore, the C_{32} 1,15 diol was found in 90% of the 62 lakes used in the global study of Rampen et al. (2014b) with 75% of the South American lakes and 30% of the European lake having the C_{32} 1,15 diol as the major diol in the sediments. Also, Castañeda et al. (2011) found that the C_{32} 1,15-diol was the major diol in lake Malawi. In contrast, in open marine environments, the C_{32} 1,15-diol is generally <20 % of the total LCDs (Rampen et al., 2014b; this study). The regions where the C_{32} 1,15-diol represents more than 20 % of the total LCDs are areas under strong riverine influence like the Hudson Bay (Rampen et al., 2014b). This suggests that riverine/freshwater eustigmatophytes produce the C_{32} 1,15-diol in much higher fractional abundances than the marine producers of LCDs.

Although further research should confirm this hypothesis, our results suggest that the C_{32} 1,15-diol is predominantly produced in rivers and may therefore potentially serve as a proxy for riverine OM input in marine environments. Currently, there is no organic proxy which solely reflects riverine OM input. For example, the BIT index contains both a soil and riverine production component (Weijers et al., 2007; Zell et al., 2014; De Jonge et al., 2015). Long chain n-alkanes are related to vegetation and soils (Eglinton and Hamilton, 1963), while the $\delta^{13}C$ and C/N ratio of bulk OM are also reflecting vegetation, soil and to some extent riverine OM (Hedges et al., 1997). The different influences on the terrigenous proxies is illustrated in our regional datasets where sometimes significant correlations between the fraction of C_{32} 1,15-diol and the BIT index or $\delta^{13}C_{OM}$ is observed (Gulf of Lion, Berau delta), but sometimes not (Kara Sea). The study of proxies reflecting different parts of terrigenous OM could potentially disentangle the input of riverine, soil and vegetation OM in the marine realm.

ACCEPTED MANUSCRIPT

4.3. Effect of riverine input on LDI

Our results indicate that the C_{32} 1,15 diol is produced in rivers and subsequently transported to coastal marine environment. This may have an impact on diol distributions in coastal marine sediments, specifically on SST determination using the LDI, since the eustigmatophytes in rivers most likely also produce LCDs other than the C_{32} 1,15 diol. We investigated this by calculating SST from the LDI using the calibration of Rampen et al. (2012) and comparing the values obtained with the satellite-derived annual mean SST (for the Gulf of Lion and Berau Delta) or annual mean SST obtained from the World Ocean Database (for the Kara Sea and Amazon shelf). Figure 8 shows the geographical distribution of this temperature difference for the different areas studied. The LDI-estimated SSTs for the Amazon shelf do not show any substantial difference with the satellite-derived SSTs, which agrees with the idea that their surface sediments are unlikely to be affected by a substantial input from the Amazon River (see the discussion above). In contrast, the LDI-SST values for the Kara Sea are much higher than observed annual mean SST (+ 0 to +11°C), with a higher difference close to the Yenisei river mouth. This may derive from a seasonal bias, i.e. the diols can be produced during a specific season and not reflect annual mean SSTs. For the subpolar Kara Sea, the diols may be more likely produced during summer time rather than winter time when the sea is frozen and light penetration for photosynthesis is limited. Indeed, when we compared the LDI-SST with summer SST, the values are much closer, between +0 to +7 °C (Fig. 8) with the highest difference found close to the river mouth and in the northern surface sediments. The higher values close to the river mouth may relate to the input of diols from the river. Indeed, there is more C_{30} 1,15-diol than 1,13-diols in the Yenisei River SPM (Fig. 2), which results in higher LDI values and, consequently, higher LDI-SST.

ACCEPTED MANUSCRIPT

For the Berau delta, the LDI-SST underestimates SST close to the Berau River mouth (Fig. 8, up to -10 °C) but is similar to the satellite-derived SST further away from the river mouth and within the ±2 °C error range of the LDI-SST calibration (Rampen et al., 2012). This is also the case for the Gulf of Lion, where the LDI-SST is lower than the satellite-derived SST close to the Rhône mouth (Fig. 8, up to -5 °C). These trends are similar to what De Bar et al. (2016) found in the Portugal margin where the SST-LDI gave colder SST-LDI values closer to the river mouth. De Bar et al. (2016) suggested that this could come from the presence of different diol producer communities in the delta region, leading to a production of diols in different proportions than those of the open marine communities. Regardless of the exact causes, our results suggest that the LDI should be used with caution in coastal, river influenced areas.

5. Conclusion

The diol distribution in surface sediments from four shelf seas from different climate regions shows that the C_{32} 1,15-diol is more abundant close to the coast and even more in rivers sediments and SPM. The relative abundance of the C_{32} 1,15-diol is also strongly positively correlated to the BIT index, a proxy for soil and riverine OM input. Together with the absence of the C_{32} 1,15-diol in soils and vegetation, this indicates that the C_{32} 1,15-diol in rivers is predominantly derived from riverine in-situ production, most likely by freshwater eustigmatophyte algae. This makes the relative abundance of the C_{32} 1,15-diol a potential proxy for tracing riverine input, both in present day environments such as river mouths as well as in marine sedimentary records of river outflows. Our study shows that riverine diols affect LDI-reconstructed SSTs in coastal seas under riverine influence.

ACCEPTED MANUSCRIPT

Acknowledgement

ACCEPTED MANUSCRIPT

We thanks Jort Ossebaar, Anchelique Mets and Denise Dorhout for analytical support, Dr. Sebastiaan Rampen for helpful discussions and Ivan Tomberg, Dr. Roselyne Buscail, Dr. Alina Stadnitskaia, Dr. Georgy Cherkashov, Dr. David Hollander, Dr. Kees Booij and Wim Boer for access to samples. We thanks three anonymous reviewers for their thoughtful comments that improved the manuscript. This research has been funded by the European Research Council (ERC) under the European Union's Seventh Framework Program (FP7/2007-2013) ERC grant agreement [339206] to SS. JSSD and SS receive funding from the Netherlands Earth System Science Center (NESSC) though a gravitation grant from the Dutch ministry for Education, Culture and Science.

ACCEPTED MANUSCRIPT

ACCEPTED MANUSCRIPT

Table 1: Pearson correlation table between the C_{32} 1,15-diol and environmental parameters for all the areas combined. SSTs are from observational data. Values in bold are significant values ($p<0.005$)

	TOC	$\delta^{13}C$	SST	BIT index	Distance*	C_{32} 1,15-diol
TOC						
$\delta^{13}C$	**-0.758**					
SST	-0.132	**-0.305**				
BIT index	**0.591**	**-0.645**	-0.123			
Distance*	-0.135	**0.517**	**-0.855**	-0.027		
C_{32} 1,15-diol	**0.608**	**-0.617**	0.001	**0.341**	-0.219	

*Distance from the closest river mouth

ACCEPTED MANUSCRIPT

ACCEPTED MANUSCRIPT

References

Arifin Z. and Koesmawati T.A. (2007) Spatial distribution of trace metals (Pb, Cr, Cu and Zn) in sediments of the Berau delta, East Kalimantan and their accumulation in benthic biota. *Mar. Res. Indonesia* **32**, 2, 89-94.

Bale N.J., Hopmans E.C., Zell C., Sobrinho R.L., Kim J-H., Sinninghe Damsté J.S., Villareal T.A. and Schouten S. (2015) Long chain glycolipids with pentose head groups as biomarkers for marine endosymbiotic heterocystous cyanobacteria. *Org. Geochem*. **81**, 1-7.

Booij K., Arifin Z. and Purbonegoro T. (2012) Perylene dominates the organic contaminant profile in the Berau delta East Kalimantan, Indonesia. *Mar. Pollut. Bull.* **64**, 1049–1054.

Boyer T.P., Antonov J. I., Baranova O. K., Coleman C., Garcia H. E., Grodsky A., Johnson D. R., Locarnini R. A., Mishonov A. V., O'Brien T.D., Paver C.R., Reagan J.R., Seidov D., Smolyar I. V., and Zweng M. M. (2013) World Ocean Database 2013, NOAA Atlas NESDIS 72, S. Levitus, Ed., A. Mishonov, Technical Ed.; Silver Spring, MD, 209.

Callede J., Kosuth P., Loup J.-L. and Santos Guimaraes V. (2000) Discharge determination by Acoustic Doppler Current Profilers (ADCP): a moving bottom error correction method and its application on the River Amazon at Óbidos. *Hydrolog. Sci. J.* **45**, 911-924.

Castaneda I.S., Werne J.P., Johnson T.C. and Powers L.A. (2011) Organic geochemical records from Lake Malawi (East Africa) of the last 700 years, part II: Biomarker evidence for recent changes in primary productivity. *Palaeogeogr. Palaeoclimatol. Palaeoecol.* **303**, 140-154.

De Bar M.W., Dorhout D.J.C., Hopmans E.C., Sinninghe Damsté J.S. and Schouten S. (2016) Constraints on the application of long chain diol proxies in the Iberian Atlantic margin. *Org. Geochem.* **101**, 184-195.

ACCEPTED MANUSCRIPT

De Jonge C., Stadnitskaia A., Hopmans E.C., Cherkashov G., Fedotov A. and Sinninghe Damsté J.S. (2014) In situ produced branched glycerol dialkyl glycerol tetraethers in suspended particulate matter from the Yenisei River, Eastern Siberia. *Geochim. Cosmochim. Acta* **125**, 476–491.

De Jonge C., Stadnitskaia A., Hopmans E.C., Cherkashov G., Fedotov A., Streletskaya I.D., Vasiliev A.A. and Sinninghe Damsté J.S. (2015a) Drastic changes in the distribution of branched tetraether lipids in suspended matter and sediments from the Yenisei River and Kara Sea (Siberia): Implications for the use of brGDGT-based proxies in coastal marine sediments. *Geochim.Cosmochim. Acta* **165**, 200-225.

De Jonge C., Stadnitskaia A., Fedotov A. and Sinninghe Damsté J.S. (2015b) Impact of riverine suspended particulate matter on the branched glycerol dialkyl glycerol tetraether composition of lakes: The outflow of the Selenga River in Lake Baikal (Russia). *Org. Geochem.* **83-84**, 241-252.

De Leeuw J.W., Rijpstra W.I.C. and Schenck P.A. (1981) The occurrence and identification of C_{30}, C_{31} and C_{32} alkan-1,15-diols and alkan-15-one-1-ols in Unit I and Unit II Black Sea sediments. *Geochim. Cosmochim. Acta,* **45,** 2281-2285.

Dunne T., Mertes L.A.K., Meade R.H., Richey J.E. and Forsberg B.R. (1998) Exchanges of sediment between the flood plain and channel of the Amazon River in Brazil. *Geol. Soc. Am. Bull.* **110**, 450-467.

Durrieu de Madron X., Abassi A., Heussner S., Monaco A., Aloisi J.C., Radakovitch O., Giresse P., Buscail R. and Kerherve P. (2000) Particulate matter and organic carbon budgets for the Gulf of Lions (NW Mediterranean). *Oceanol. Acta* **23**, 717-730.

Eglinton G. and Hamilton R.J. (1963) *The Distribution of Alkanes, In Chemical Plant Taxonomy*, Academic Press, 187-217.

ACCEPTED MANUSCRIPT

Gelin F., Boogers I., Noordeloos A.A.M., Sinninghe Damsté J.S., Riegman R. and de Leeuw J.W. (1997) Resistant biomacromolecules in marine microalgae of the classes Eustigmatophyceae and Chlorophyceae: geochemical implications. *Org. Geochem*. **26**, 659–67.

Gogou A. and Stephanou E.G. (2004) Marine organic geochemistry of the Eastern Mediterranean: 2. Polar biomarkers in Cretan Sea surficial sediments. *Mar. Chem.* **85**, 1-25.

Goulding M., Barthem R. and Ferreira E. (2003) *The Smithsonian Atlas of the Amazon* Smithsonian Books, Washington DC, 255.

Harger J.R.E. (1995) Air-temperature variation and ENSO effects in Indonesia, The Philippines and El Salvador. ENSO pattern and changes from 1866-1993 *Atm. Environ.,* **29**, 1919-1942.

Hedges J.I., Keil R.G. and Benner R. (1997) What happens to terrestrial organic matter in the ocean? *Org. Geochem.* **27**, 195–212.

Hopmans E.C., Weijers J.W.H., Schefuß E., Herfort L., Sinninghe Damsté J.S. and Schouten S. (2004) A novel proxy for terrestrial organic matter in sediments based on branched and isoprenoid tetraether lipids. *Earth Planet. Sci. Lett*. **224**, 107-116.

Jetter R, Riederer M., Seyer A. and Mioskowski C. (1996) Homologous long-chain alkanediols from Papaver leaf cuticular waxes. *Phytochem.* **42,** 1617–1620.

Jetter R. and Riederer M. (1999) Long-chain alkanediols, ketoaldehydes, ketoalcohols and ketoalkyl esters in the cuticular waxes of *Osmunda regalis* fronds. *Phytochem.* **52**, 907–915.

Jetter R. (2000) Long-chain alkanediols from *Myricaria germanica* leaf cuticular waxes. *Phytochem.* **55**, 169–176.

ACCEPTED MANUSCRIPT

Kim J.-H., Schouten S., Buscail R., Ludwig W., Bonnin J., . Sinninghe Damsté J.S. and Bourrin F. (2006) Origin and distribution of terrestrial organic matter in the NW Mediterranean (Gulf of Lions): exploring the newly developed BIT index Geochemistry. *Geochem. Geophys*. *Geosyst*. **7**,1–20.

Kim J.-H., Ludwig W., Schouten S., Kerherv P., Herfort L., Bonnin J. and Sinninghe Damsté J.S. (2007) Impact of flood events on the transport of terrestrial organic matter to the ocean: a study of the Têt River (SW France) using the BIT index. *Org. Geochem*. **38**, 1593–1606.

Kim J.-H., Zarzycka B., Buscail R., Peterse F., Bonnin J., Ludwig W., Schouten S. and Sinninghe Damsté J.S. (2010) Contribution of river-borne soil organic carbon to the Gulf of Lions (NW Mediterranean). *Limnol. Oceanogr.* **55**, 2, 507-518.

Kim J.-H., Moreira-Turq P., Pérez M.A.P., Abril G., Mortillaro J.-M., Weijers J.W.H., Meziane T. and Sinninghe Damsté J.S. (2012) Tracing soil organic carbon in the lower Amazon River and its tributaries using GDGT distributions and bulk organic matter properties. *Geochim. Cosmochim. Acta* **90**, 163–180.

Kim J.-H., Buscail R., Fanget A.-S., Eyrolle-Boyer F., Bassetti M.-A., Dorhout D., Baas M., Berné S. and Sinninghe Damsté J.S. (2014) Impact of river channel shifts on tetraether lipids in the Rhône prodelta (NW Mediterranean): Implication for the BIT index as an indicator of palaeoflood events. *Org. Geochem*. **75**, 99-108.

Kim J.-H., Schouten S., Rodrigo-Gamiz M., Rampen S.W., Marino G., Huguet C., Helmke P., Buscail R., Hopmans E.C., Pross J., Sangiorgi F., Middelburg J.B.M. and Sinninghe Damsté J.S. (2015) Influence of deep-water derived isoprenoid tetraether lipids on the TEX_{86}^{H}paleothermometer in the Mediterranean Sea. *Geochim. Cosmochim. Acta* **150**, 125-141.

ACCEPTED MANUSCRIPT

Lammers R.B. and Shiklomanov A.I (2000) R-ArcticNet, A Regional Hydrographic Data Network for the Pan-Arctic Region, Durham, NH: Water Systems Analysis Group, University of New Hampshire; distributed by the National Snow and Ice Data Center.

Méjanelle L., Sanchez-Gargallo A., Bentaleb I. and Grimalt J.O. (2003) Long chain n-alkyl diols, hydroxy ketones and sterols in a marine eustigmatophyte, *Nannochloropsis gaditana*, and in *Brachionus plicatilis* feeding on the algae. *Org. Geochem.***34,** 527–538.

Meyers P. A. (1994) Preservation of elemental and isotopic source identification of sedimentary organic matter. *Chem. Geol*. **114**, 289–302.

Milliman J.D. and Meade R.H. (1983) World-wide delivery of river sediment to the oceans. *J. Geol.* **91**, 1–21.

New M., Lister D., Hulme M. and Makin I. (2002) A high resolution data set of surface climate over global land areas. *Clim. Res.* **21**, 1–25.

Olivier J.-M., Carre G., Lamouroux N., Dole-Olivier M.-J., Malard F., Bravard J.-P. and Amoros C. (2009) Chapter 7 – the Rhône River basin," in River of Europe, eds K. Tockner, U. Uehlinger, C. T. Robinson (Amsterdam: Academic Press), 247–295.

Peterse F., Kim J.-H., Schouten S., Klitgaard Kristensen D., Koç N. and Sinninghe Damsté J.S. (2009) Constraints on the application of the MBT–CBT palaeothermometer at high latitude environments (Svalbard, Norway). *Org. Geochem*. **40**, 692–699.

Peterse F., Hopmans E.C., Schouten S., Mets A., Rijpstra W.I.C. and Sinninghe Damsté J.S. (2011) Identification and distribution of intact polar branched tetraether lipids in peat and soil. *Org. Geochem.* **42**, 1007–1015.

ACCEPTED MANUSCRIPT

Pitcher A., Hopmans E.C., Schouten S. and Sinninghe Damsté J.S. (2009) Separation of core and intact polar archaeal tetraether lipids using silica columns: insights into living and fossil biomass contributions. *Org. Geochem.* **40**, 12–19.

Plancq J., Grossi V., Pittet B., Huguet C., Rosell-Melé A. and Mattioli E. (2015) Multi-proxy constraints on sapropel formation during the late Pliocene of central Mediterranean (southwest Sicily). *Earth Planet. Sci. Lett.* **420**, 30-44.

Rampen S.W., Schouten.S., Wakeham S.G. and Sinninghe Damsté J.S. (2007) Seasonal and spatial variation in the sources and fluxes of long chain diols and mid-chain hydroxy methyl alkanoates in the Arabian Sea. *Org. Geochem.* **38**, 165–179.

Rampen S.W., Schouten S., Koning E., Brummer G.-J.A. and Sinninghe Damsté J.S. (2008) A 90 kyr upwelling record from the northwestern Indian Ocean using a novel long-chain diol index. *Earth Planet. Sci. Lett.* **276**, 207–213.

Rampen S.W., Shouten S. and Sinninghe Damsté J.S. (2011) Occurrence of long chain 1,14 diols in *Apedinella radians*. *Org. Geochem.* **42**, 572–574.

Rampen S.W., Willmott V., Kim J.-H., Uliana E., Mollenhauer G., Schefuß E., Sinninghe Damsté J.S. and Schouten S. (2012) Long chain 1,13- and 1,15-diols as a potential proxy for palaeotemperature reconstruction. *Geochim. Cosmochim. Acta* **84**, 204–216.

Rampen S.W., Willmott V., Kim J-H., Rodrigo-Gámiz M., Uliana E., Mollenhauer G., Schefuß E., Sinninghe Damsté J.S. and Schouten S. (2014a) Evaluation of long chain 1,14-alkyl diols in marine sediments as indicators for upwelling and temperature. *Org. Geochem.* **76**, 39-47.

ACCEPTED MANUSCRIPT

Rampen S.W., Datema M., Rodrigo-Gámiz M., Schouten S., Reichart G.-J. and Sinninghe Damsté J.S. (2014b) Sources and proxy potential of long chain alkyl diols in lacustrine environments. *Geochim. Cosmochim. Acta* **144**, 59-71.

Romero-Viana L., Kienel U. and Sachse D. (2012) Lipid biomarker signatures in a hypersaline lake on Isabel Island (Eastern Pacific) as a proxy for past rainfall anomaly (1942–2006 AD). *Palaeogeogr. Palaeoclimatol. Palaeoecol.* **350–352**, 49–61.

Sabatier P., Maillet G., Provansal M., Fleury T.J., Suanez S. and Vella C. (2006) Sediment budget of the Rhône delta shoreface since the middle of the 19th century. *Mar. Geol.* **234**, 143–157.

Schmidt F., Hinrichs K.-U. and Elvert M. (2010) Sources, transport, and partitioning of organic matter at a highly dynamic continental margin. *Mar. Chem.* **118** 37-55.

Shimokwara M., Nishimura M., Matsuda T., Akiyama N. and Takayoshi K. (2010) Bound forms, compositional features, major sources and diagenesis of long chain, alkyl mid-chain diols in Lake Baikal sediments over the past 28,000 years. *Org. Geochem*. **41**, 753–766.

Sinninghe Damsté J.S., Rijpstra. W.I.C., Abbas B., Muyzer G. and Schouten S. (2003) A diatomaceous origin for long-chain diols and mid-chain hydroxy methyl alkanoates widely occurring in Quaternary marine sediments: indicators for high nutrient conditions. *Geochim. Cosmochim. Acta* **67**, 1339–1348.

Sinninghe Damsté J.S. (2016) Spatial heterogeneity of sources of branched tetraethers in shelf systems: The geochemistry of tetraethers in the Berau River delta (Kalimantan, Indonesia). *Geochim. Cosmochim. Acta*. **186**, 13-31.

Sparkes R.B., Selver A.D., Bischoff J., Talbot H.M., Gustafsson O., Semiletov I.P., Dudarev O.V. and van Dongen B.E. (2015) GDGT distributions on the East Siberian Arctic Shelf: Implications for organic carbon export, burial and degradation *Biogeosci*. **12**, 3753–3768.

ACCEPTED MANUSCRIPT

Speelman E.N., Reichart G.-J., de Leeuw J.W., Rijpstra. W.I.C. and Sinninghe Damsté J.S. (2009) Biomarker lipids of the freshwater fern *Azolla* and its fossil counterpart from the Eocene Arctic. *Org. Geochem.* **40**, 628–637.

Telang S. A., Pocklington R., Naidu A. S., Romankevich E. A., Gitelson I. I. and Gladyshev M. I. (1991) Carbon and mineral transport in major North American, Russian, and Siberian rivers: the St Lawrence, the Mackenzie, the Yukon, the Arctic Alaskan rivers, the Arctic Basin rivers, and the Yenisei. In *Biogeochemistry of Major World Rivers* (eds. Degens E.T., Kempe S. and Richey J.E.), Wiley & Sons., Chichester, pp. 75–104.

Thill A., Moustier S., Garnier J.-M., Estournel C., Naudin J.-J. and Bottero J.-Y. (2001) Evolution of particle size and concentration in the Rhone river mixing zone: Influence of salt flocculation. *Cont. Shelf Res.* **21**, 2127-2140.

Versteegh G.J.M., Bosch H.J. and de Leeuw J.W. (1997) Potential palaeoenvironmental information of C_{24} to C_{36} mid-chain diols, keto-ols and mid-chain hydroxy fatty acids; A critical review. *Org. Geochem*. **27,** 1–13.

Versteegh G.J.M., Jansen J.H.F., de Leeuw J.W. and Schneider R.R. (2000) Mid-chain diols and keto-ols in SE Atlantic sediments: A new tool for tracing past sea surface water masses? *Geochim. Cosmochim. Acta* **64**, 1879–1892.

Villanueva L., Besseling M., Rodrigo-Gámiz M., Rampen S.W., Verschuren D. and Sinninghe Damsté J.S. (2014) Potential biological sources of long chain alkyl diols in a lacustrine system. *Org. Geochem.* **68,** 27–30.

Volkman J.K., Barrett S.M., Dunstan G.A. and Jeffrey S.W. (1992) C_{30}–C_{32} alkyl diols and unsaturated alcohols in microalgae of the class *Eustigmatophyceae*. *Org. Geochem.* **18** , 131–138.

ACCEPTED MANUSCRIPT

Volkman J.K., Barrett S.M. and Blackburn S.I. (1999) Eustigmatophyte microalgae are potential sources of C_{29} sterols, C_{22}–C_{28} n-alcohols and C_{28}–C_{32} n-alkyl diols in freshwater environments. *Org. Geochem.* **30**, 307–318.

Walsh E.M., Ingalls A.E. and Keil R.G. (2008) Sources and transport of terrestrial organic matter in Vancouver Island fjords and the Vancouver–Washington Margin: A multiproxy approach using $\delta^{13}C_{org}$, lignin phenols, and the ether lipid BIT index. *Limnol. Oceanogr.* **53**, 1054–1063.

Weijers J.W.H., Schouten S., Van den Donker J.C., Hopmans E.C. and Sinninghe Damsté J.S. (2007) Environmental controls on bacterial tetraether membrane lipid distribution in soils. *Geochim. Cosmochim. Acta* **71**, 703–713.

Willmott V., Rampen S.W., Domack E., Canals M., Sinninghe Damsté J.S. and Schouten S. (2010) Holocene changes in *Proboscia* diatom productivity in shelf waters of the north-western Antarctic Peninsula. *Antarct. Sci.* **22**, 3–10.

Zell C., Kim J.-H., Moreira Turq P., Abril G., Hopmans E.C., Bonnet M.-P., Lima Sobrinho R. and Sinninghe Damsté J.S. (2013a) Disentangling the origins of branched tetraether lipids and crenarchaeol in the lower Amazon River: implications for GDGT-based proxies. *Limnol. Oceanogr.* **58**, 343–353.

Zell C., Kim J.-H., Abril G., Lima Sobrinho R., Dorhout D., Moreira Turq P. and Sinninghe Damsté J.S. (2013b) Impact of seasonal hydrological variation on the distributions of tetraether lipids along the Amazon River in the central Amazon basin: implications for the MBT/CBT paleothermometer and the BIT index. *Front. Microbiol*. **4**, doi:10.3389/fmicb.2013.00228.

Zell C., Kim J.-H., Hollander D., Lorenzoni L., Baker P., Guizan Silva C., Nittrouer C. and Sinninghe Damsté J.S. (2014) Sources and distributions of branched and isoprenoid tetraether lipids on the Amazon shelf

ACCEPTED MANUSCRIPT

and fan: Implications for the use of GDGT-based proxies in marine sediments. *Geochim. Cosmochim. Acta* **139**, 293-312.

Zhang Z., Metzger P. and Sachs J.P. (2011) Co-occurrence of long chain diols, keto-ols, hydroxy acids and keto acids in recent sediments of Lake El Junco Galapagos Islands. Org. Geochem. 42, 823–837.

ACCEPTED MANUSCRIPT

ACCEPTED MANUSCRIPT

Figure legends

Figure 1 Location of the study sites. Surface sediments and suspended particulate matter are represented by red circles, soil samples are represented by blue squares.

Figure 2 Average diol (C_{28} 1,13, C_{28} 1,14, C_{32} 1,15, C_{30} 1,13, C_{30} 1,14 and C_{30} 1,15) distributions for the four coastal areas studied. Distributions for both surface sediments and riverine suspended particulate matter (when available) are given. Error bars indicate the standard deviations and n is the number of samples for each location.

Figure 3 Spatial distribution of the relative abundance of the six diols studied (C_{28} 1,13, C_{28} 1,14, C_{32} 1,15, C_{30} 1,13, C_{30} 1,14 and C_{30} 1,15) and, for comparison, the BIT index (from Kim et al. 2006, 2015) in the surface sediments of the Gulf of Lion (the southernmost site has been excluded). The map was made by Ocean Data View software, using DIVA gridding.

Figure 4 Spatial distribution of the relative abundance of the six diols studied (C_{28} 1,13, C_{28} 1,14, C_{32} 1,15, C_{30} 1,13, C_{30} 1,14 and C_{30} 1,15) and, for comparison, the BIT index (from Kim et al. 2012, Zell et al., 2013a, 2013b) in the surface sediments of the Amazon shelf. The map was made by Ocean Data View software, using DIVA gridding.

Figure 5 Spatial distribution of the relative abundance of the six diols studied (C_{28} 1,13, C_{28} 1,14, C_{32} 1,15, C_{30} 1,13, C_{30} 1,14 and C_{30} 1,15) and, for comparison, the BIT index (from De Jonge et al. 2014, 2015a) in the surface sediments of the Kara Sea. The map was made by Ocean Data View software, using DIVA gridding.

ACCEPTED MANUSCRIPT

Figure 6 Spatial distribution of the relative abundance of the six diols studied (C_{28} 1,13, C_{28} 1,14, C_{32} 1,15, C_{30} 1,13, C_{30} 1,14 and C_{30} 1,15) and, for comparison, the BIT index (from Sinninghe Damsté, 2016) in the surface sediments of the Berau delta. The map was made by Ocean Data View software, using DIVA gridding.

Figure 7 PCA on the relative abundances of C_{28} 1,13, C_{28} 1,14, C_{30} 1,13, C_{30} 1,14, C_{30} 1,15 and C_{32} 1,15 for four coastal regions (Gulf of Lion, Amazon shelf, Kara Sea and Berau delta) for (a) surface sediments and (b) riverine suspended particulate matter.

Figure 8 Difference between satellite-derived SST and SST estimated from the LDI for the Gulf of Lion, Berau delta, Amazon shelf and Kara Sea. The map was made by Ocean Data View software, using DIVA gridding.

ACCEPTED MANUSCRIPT

Figure 1

ACCEPTED MANUSCRIPT

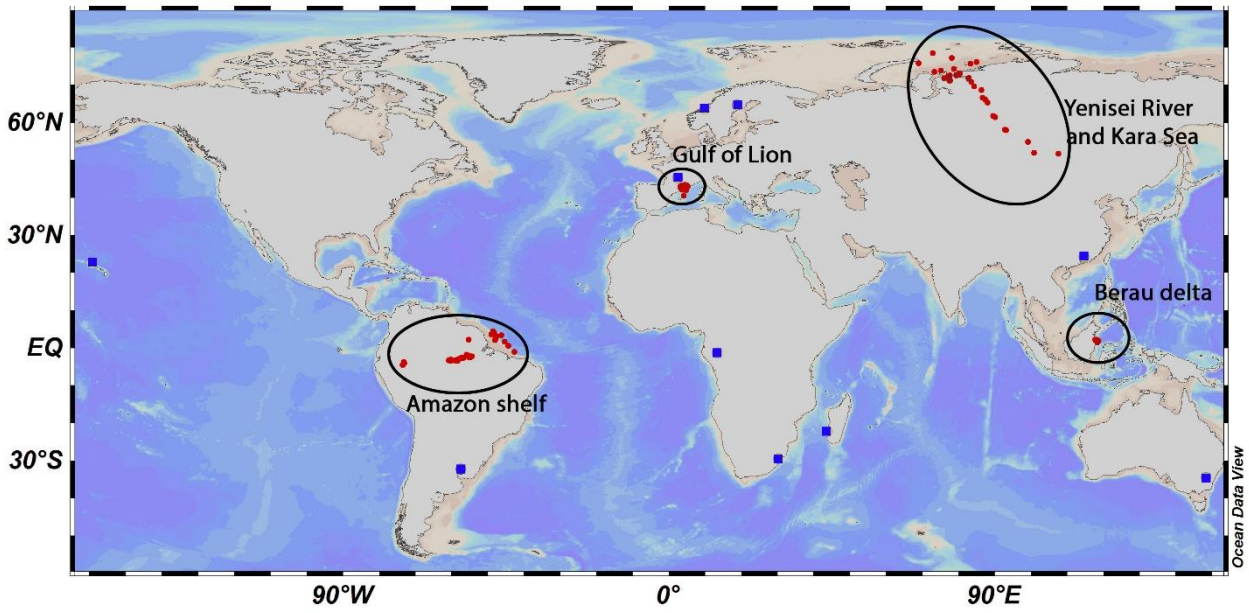

ACCEPTED MANUSCRIPT

Figure 2

ACCEPTED MANUSCRIPT

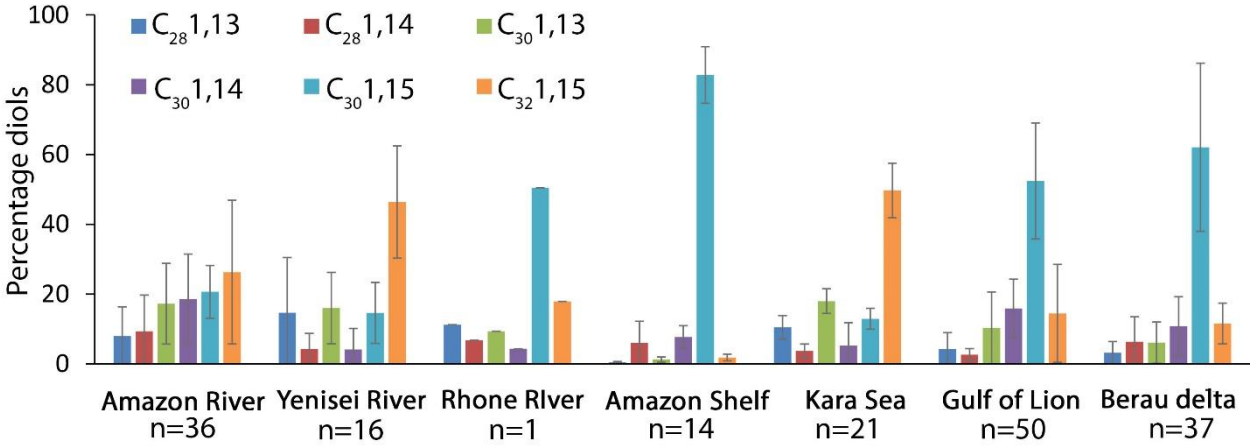

ACCEPTED MANUSCRIPT

Figure 3

ACCEPTED MANUSCRIPT

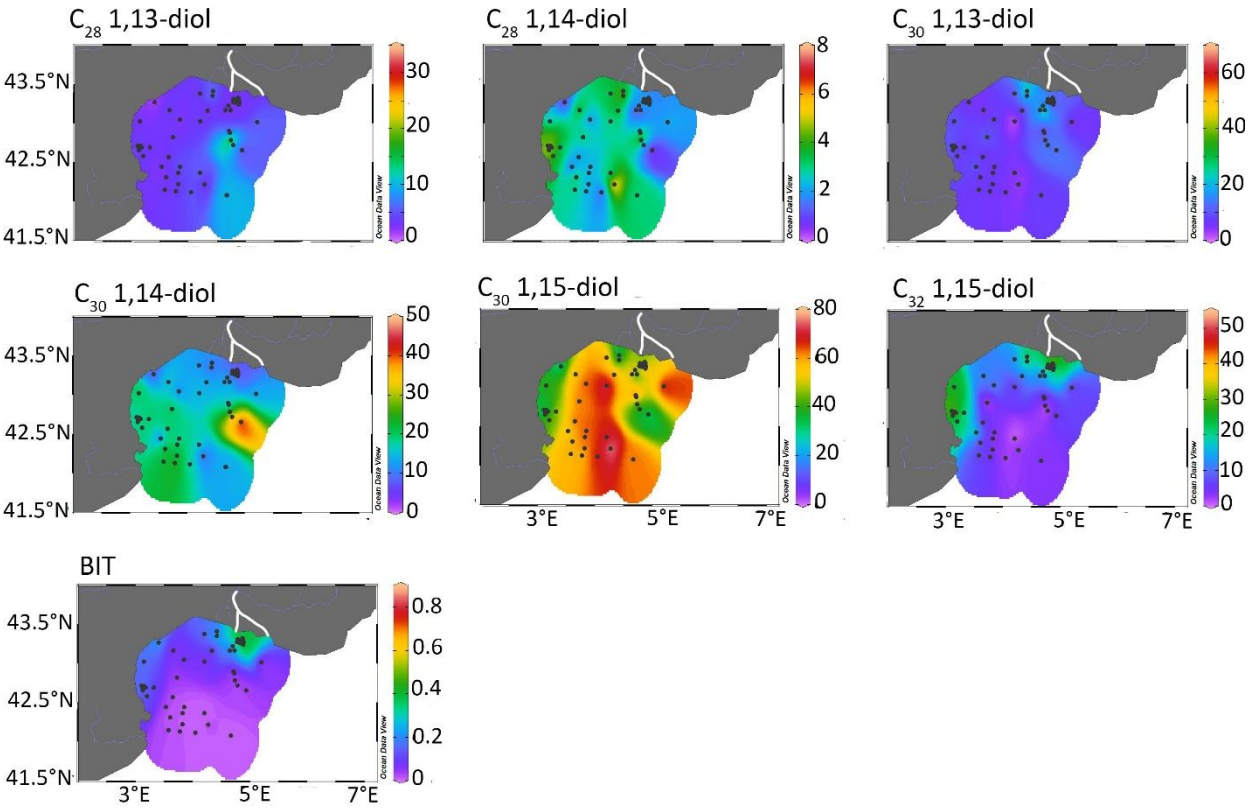

Figure 4

ACCEPTED MANUSCRIPT

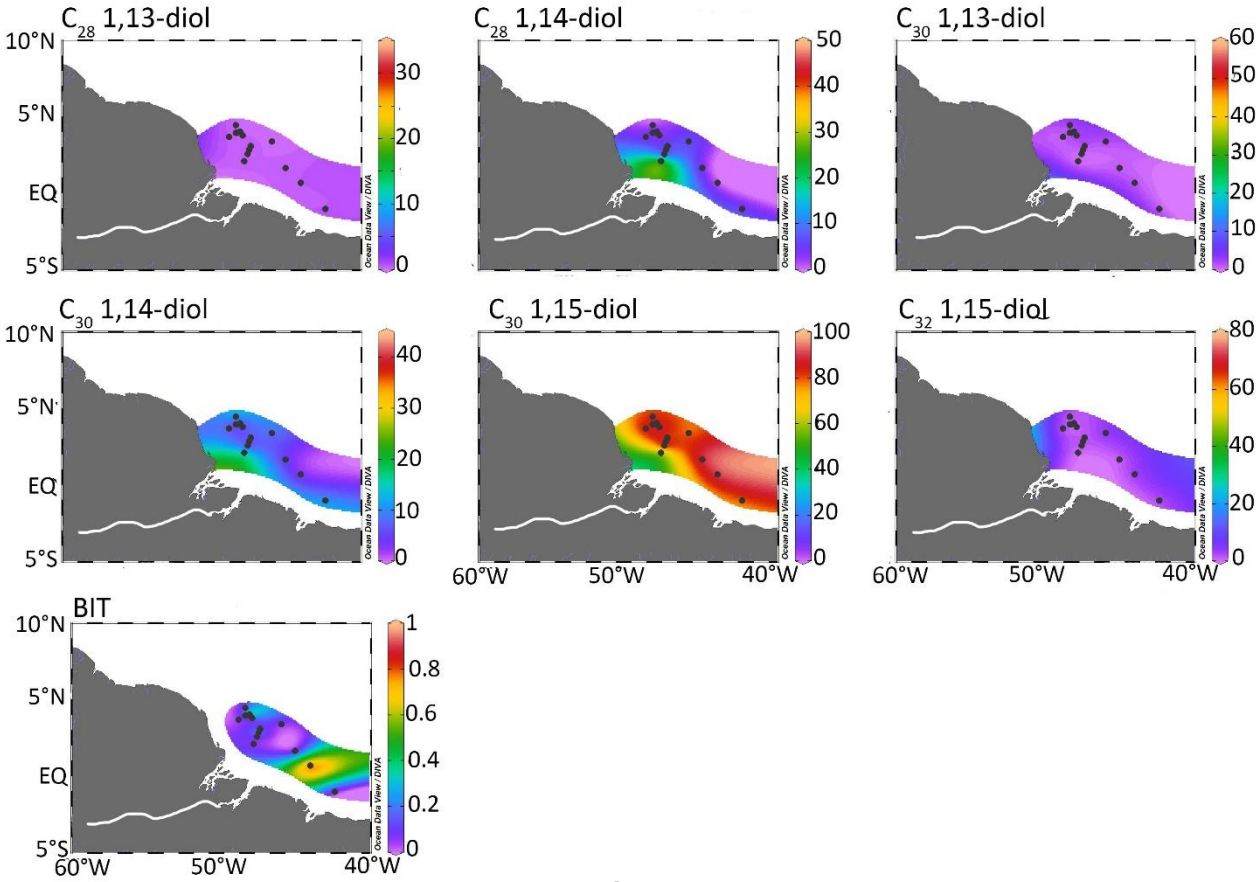

ACCEPTED

Figure 5

ACCEPTED MANUSCRIPT

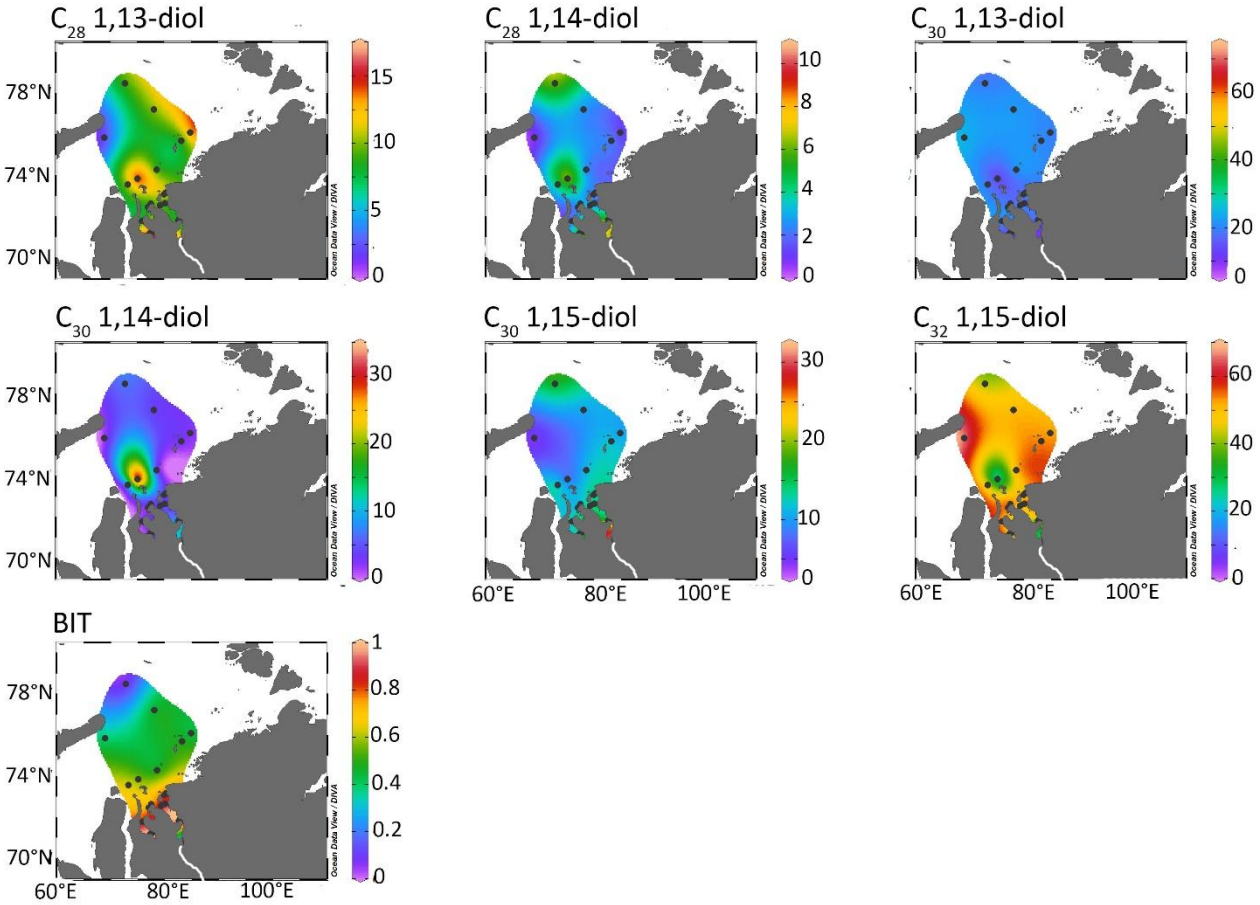

ACCEPTED

Figure 6

ACCEPTED MANUSCRIPT

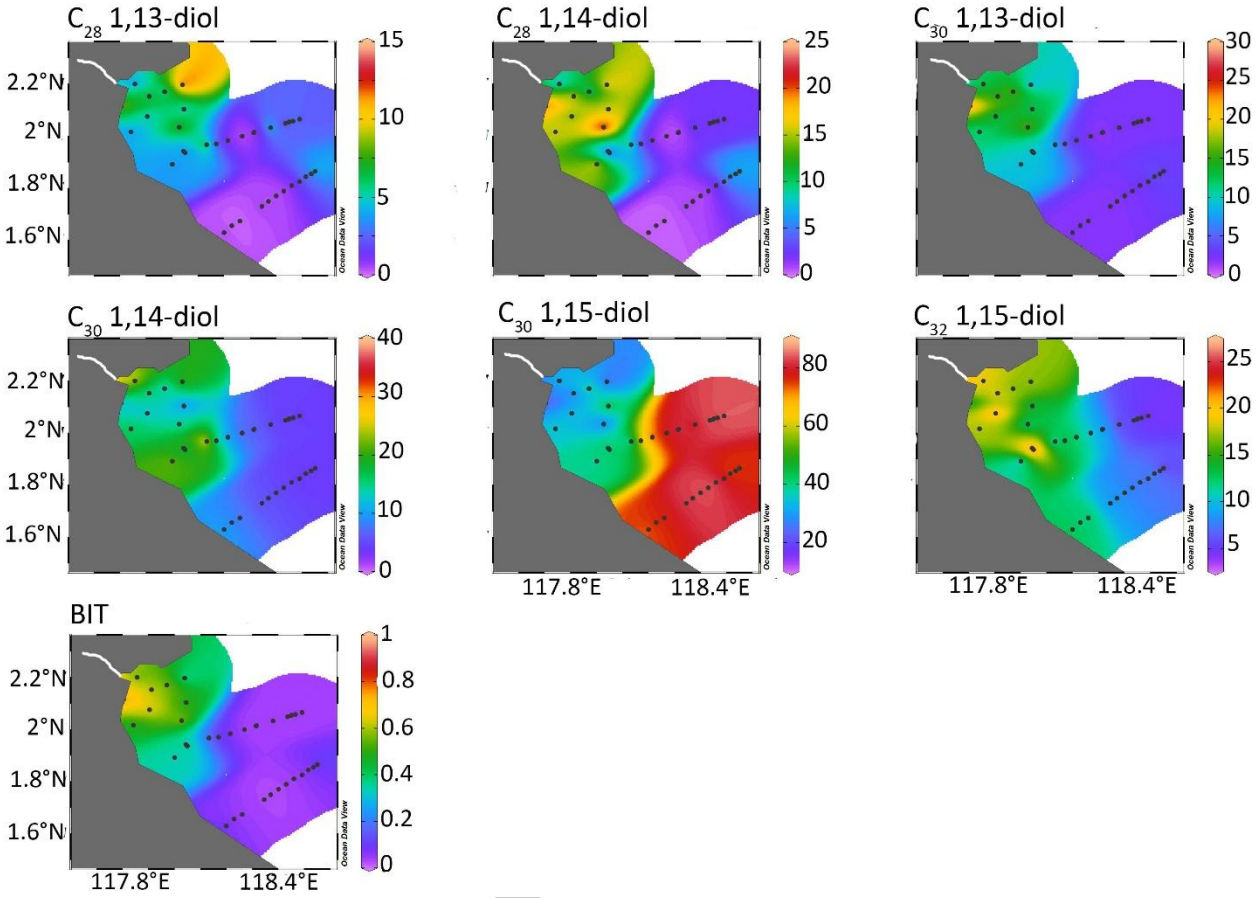

ACCEPTED

Figure 7

ACCEPTED MANUSCRIPT

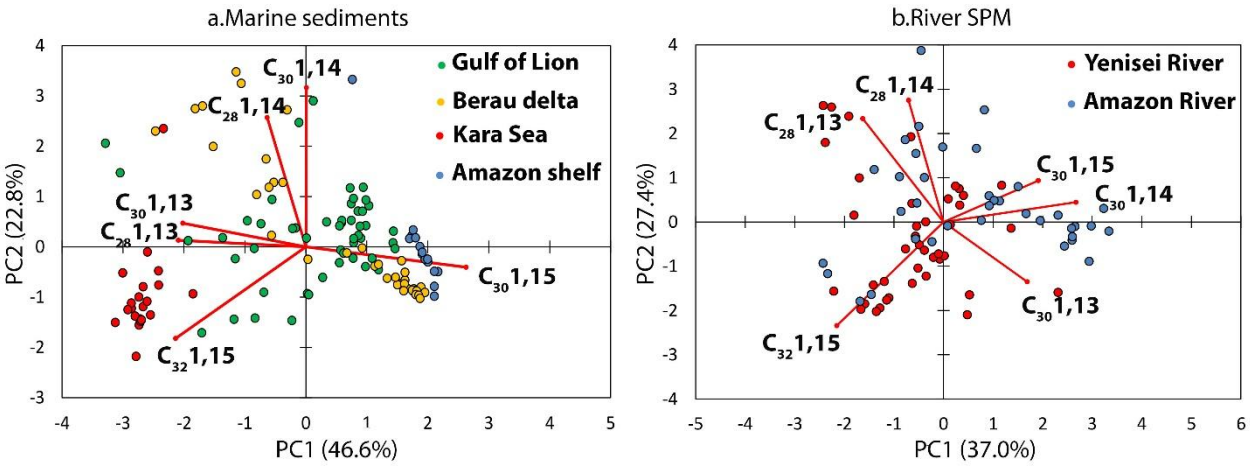

Figure 8

ACCEPTED MANUSCRIPT

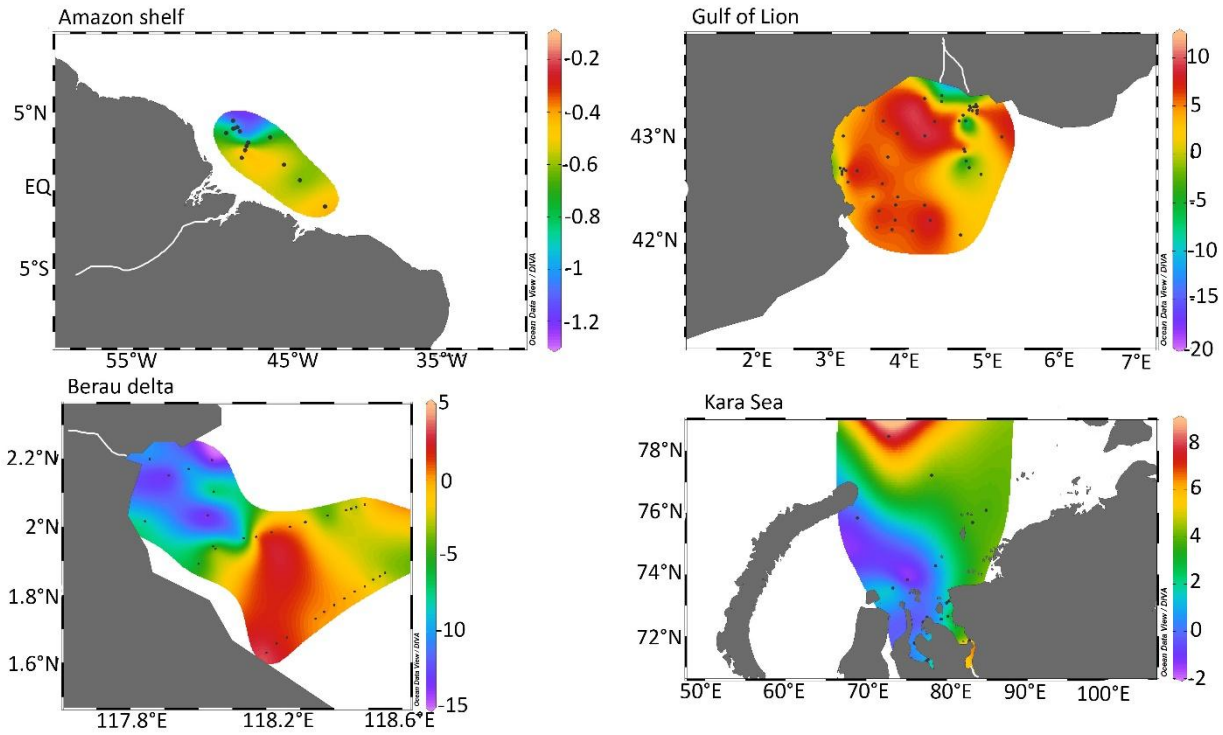

ACCEPTED MANUSCRIPT